

Superconductor-insulator phase transition in single-crystal $\text{La}_{2-x}\text{Sr}_x\text{CuO}_4$ films grown by the liquid-phase epitaxy method

A. T. M. Nazmul Islam,^{1,2,*} T. Hitosugi,³ E. Dudzik,² T. Hasegawa,³ S. Ueda,⁴ Y. Takano,⁴ F. N. Islam,⁵ M. K. R. Khan,⁵ M. N. Islam,⁵ A. K. M. A. Islam,⁵ S. Watauchi,¹ and I. Tanaka¹

¹*Center for Crystal Science and Technology, University of Yamanashi, 4008511 Kofu, Japan*

²*Helmholtz-Zentrum-Berlin für Materialien und Energie, Glienicker Strasse 100, 14109 Berlin, Germany*

³*Department of Chemistry, University of Tokyo, 1130033 Tokyo, Japan*

⁴*National Institute for Materials Science, 1-2-1 Sengen, 3050047 Tsukuba, Japan*

⁵*Department of Physics, Rajshahi University, 6205 Rajshahi, Bangladesh*

(Received 13 May 2009; revised manuscript received 10 June 2009; published 9 July 2009)

We have studied epitaxial strain effect on superconductivity in single-crystal $\text{La}_{2-x}\text{Sr}_x\text{CuO}_4$ films grown by liquid-phase epitaxy method on (001) La_2CuO_4 substrates. Due to lattice mismatch the as-grown films suffer a compressive strain in the c axis and an orthorhombic tensile strain on the ab plane with almost no relaxation up to several micrometers thickness. Our results show that $\text{La}_{2-x}\text{Sr}_x\text{CuO}_4$ ($0.10 \leq x \leq 0.15$), which is superconducting in the bulk at low temperatures, transforms to an insulating state under such strain.

DOI: [10.1103/PhysRevB.80.024505](https://doi.org/10.1103/PhysRevB.80.024505)

PACS number(s): 74.20.Mn, 74.78.Bz, 81.15.Lm

I. INTRODUCTION

The effect of lattice strain on high- T_c superconductors, for example, $\text{La}_{2-x}\text{Sr}_x\text{CuO}_4$ (LSCO) is a field of intensive research. It was found that the uniaxial strain derivatives of superconducting critical temperature T_c , $\frac{\partial T_c}{\partial \varepsilon_c}$, and $\frac{\partial T_c}{\partial \varepsilon_{ab}}$, where ε_c and ε_{ab} are strain along the c axis and ab plane, respectively, have opposite signs. This implies a compressive strain in c axis and tensile along the ab plane adds up to increase in T_c and vice versa. So, hydrostatic pressure would mostly cancel out the strain effect on T_c . In contrast, as demonstrated in several works anisotropic strain such as uniaxial pressure on bulk $\text{La}_{2-x}\text{Sr}_x\text{CuO}_4$ LSCO,^{1,2} growth of epitaxial films on suitable substrates,³⁻⁷ molecular substitution, etc., show substantial effect on T_c . An anisotropic lattice strain by molecular substitution effect, for example, Nd doping in LSCO, was found responsible for a competing static stripe phase, and hence complete destruction of superconductivity in this system.⁸⁻¹⁰ Although there are several works on epitaxial strain on LSCO showing significant variation in T_c , there are none showing complete suppression of superconductivity. This led us to believe that the methods used in previous works had limitations and with appropriate strain engineering of LSCO new phenomena could be observed.

In this work we have grown single-crystal LSCO films with different compositions and thicknesses on La_2CuO_4 (001) substrates by a method known as liquid-phase epitaxy (LPE), where films are grown from high-temperature melt. To our knowledge this is the first approach to study strain effect on superconductivity using LPE films, as all other film growth processes use vapor-phase epitaxy.³⁻⁷ We present x-ray diffraction measurements, temperature dependence of resistivities, and low-field temperature dependence of dc magnetization measurements on films with compositions $0.08 \leq x \leq 0.15$ and thicknesses from 0–30 μm . Our work demonstrates that LSCO, with superconductivity in bulk, crosses over to an insulating state in the films under epitaxial strain in films with $0.01 \leq x \leq 0.15$. Second, the films grown by LPE method are unique as they have very low thickness

dependence of strain relaxation up to several micrometers. Epitaxial strain as a control parameter for superconductor-insulator transition would in fact open up the possibility of studying the electronic and magnetic ground state under the superconducting dome in pure undoped LSCO.

II. EXPERIMENT

$\text{La}_{2-x}\text{Sr}_x\text{CuO}_4$ films with different compositions were grown by liquid-phase epitaxy method on La_2CuO_4 (001) substrates. The experimental setup for the film growth is different from a conventional process as a four-mirror-type floating-zone furnace having halogen lamps (Crystal Systems, Inc.) was used instead of a conventional furnace as heat source. No crucible was used in this process, instead a sintered rod of La_2CuO_4 (diameter of ~ 10 mm) was attached to the lower shaft to provide support to the solvent in the growth stage. The substrate was attached to the upper shaft using an alumina rod and placed at a position in the heated zone where the temperature gradient is steep. When the solvent melts completely the lower shaft is raised to allow the melt to touch the substrate to form a molten zone in between the substrate and the LCO-sintered rod. The molten zone was stirred by counter rotation of upper and lower shafts at 30–50 rpm for few minutes. The growth was then performed by pulling the substrate upward at 1.0 mm/h for 0–120 s. After the growth, the molten zone was separated from the substrate by moving the lower shaft downward. We found that popular choices of substrates such as SrTiO_3 , LaSrAlO_4 , etc., are transparent and hence difficult to heat up using IR light from halogen lamps, which can lead to quenching of molten solvent when touched with substrate. On the other hand LSCO is easy to heat up with halogen lamps. Since there is a systematic anisotropic change in lattice parameters with Sr doping in LSCO,¹¹ i.e., the c -axis lattice parameter increases while the a - (and b -) axis lattice parameter decreases, an undoped La_2CuO_4 (001) substrate is chosen to apply an in-plane tensile strain on LSCO films. We have grown cigar-shaped La_2CuO_4 single crystals by the

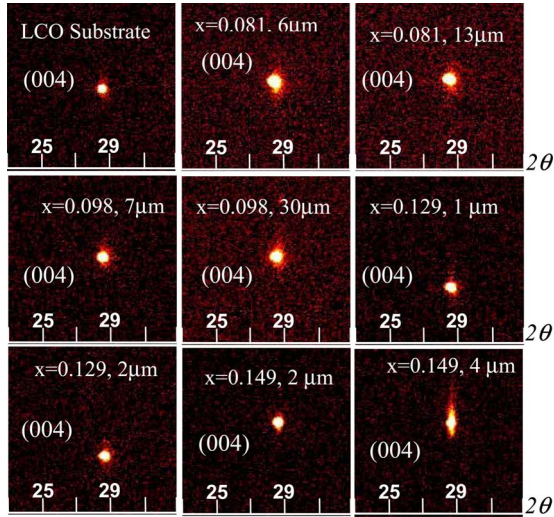


FIG. 1. (Color online) 2D image of x-ray diffraction showing (004) spots for LSCO liquid-phase epitaxial films with different compositions and thicknesses.

traveling-solvent floating-zone method, cut to the *ab* plane with thickness about 1 mm and polished mechanically to use as substrates. The solvents used for film growth were compositions of 85 mol% CuO–15 mol% $\text{La}_{2-x}\text{Sr}_x\text{O}_{3-\delta}$ ($0.2 \leq x \leq 0.6$), prepared by normal sintering method. The remnant flux frozen on top of the as-grown films were polished off. The single-crystal films were then polished to different thicknesses determined from their cross sections. Each film was checked by polarized optical microscope and scanning electron microscope and found to be free from any inclusions or grain boundaries and a straight film-substrate interface which suggests minimal melting of substrate. The compositions of the films were measured by quantitative electron probe microanalysis (EPMA) (Jeol Ltd. Model JXA8200). We realized that the accuracy of oxygen contents determined in this process may not be reliable. Nevertheless the oxygen stoichiometry in LSCO films is function of growth atmosphere. It was reported that fast cooling of film after growth in ambient oxygen is critical to eliminate excess oxygen intercalations whereas films cooled down in ozone or a mixture of ozone and molecular oxygen contains excess oxygen.^{5,6} So, in our experiments the films were cooled down at a fast rate (>20 °C/min) in flowing oxygen atmosphere to obtain LSCO with stoichiometric oxygen content. Characteristics of the epitaxial growth such as orientation of films, level of strain, etc., were examined by x-ray diffractions analysis (Bruker Model D8 Discovery).

III. RESULTS AND DISCUSSION

The compositions of the LSCO films determined by quantitative EPMA were found to have good oxygen stoichiometry and Sr contents $x=0.081$, 0.099, 0.129, and 0.149, respectively, which is almost homogeneity across the (001) plane. Figure 1 shows two-dimensional (2D) images from the x-ray diffraction analysis of the (004) peaks of liquid-phase epitaxial films with different compositions and thick-

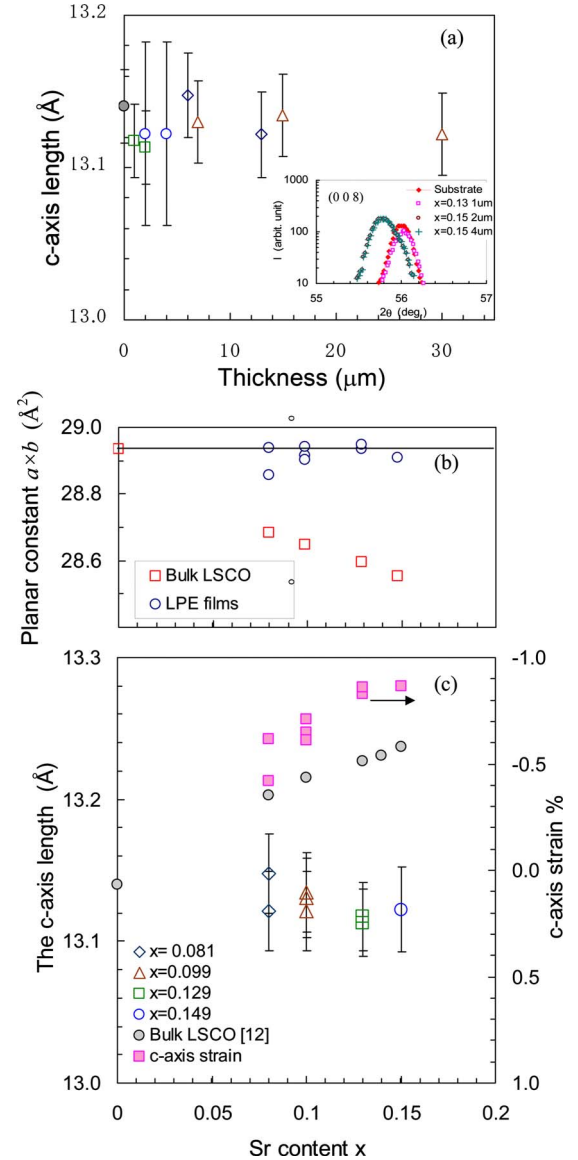


FIG. 2. (Color online) (a) The *c*-axis lattice parameters of LPE films as a function of thickness. (c) The *c*-axis lattice constant as a function of Sr content (lower panel) in comparison to bulk LSCO. The *c*-axis strain is shown in the secondary y axis (■). (b) Calculated planar constant ($a \times b$) of the LPE films compared to that of bulk LSCO.

nesses. We observe low dispersion of spots with thicknesses and no secondary spot for thinner films because of nice overlapping of spots from film and substrate, within the resolution of the instrument. Information from the x-ray diffraction measurements is summarized in Fig. 2. We observe that the *c*-axis lattice constants of films are almost independent of thicknesses [Fig. 2(a)] and compositions [Fig. 2(c)] and coincide with that of the substrate. The error bars on the *c*-axis lattice parameters represent the full width at half maximum of the (0 0 *l*) peaks, which are similar in films and LCO substrate (~ 0.02 Å) (except in $x=0.149$ films). Considering that the estimated penetration of x-ray ($\lambda=1.54056$) in the sample is ~ 5 μm, the error bars indicates the maximum dislocations in film and substrate in this thickness. The large

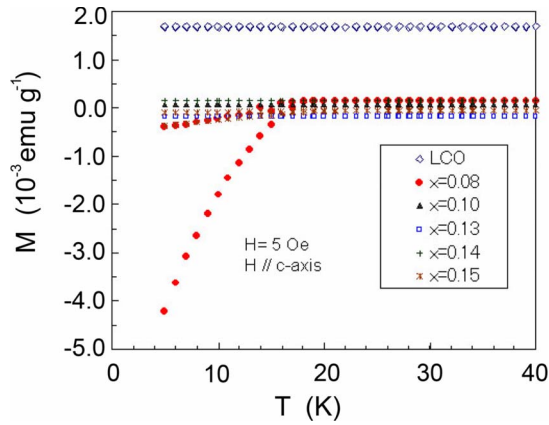


FIG. 3. (Color online) Temperature dependence of magnetization of LSCO films of different compositions.

error bar for $x=0.15$ film is due to some misfit dislocations as shown in Fig. 2(a) inset. A comparison of the c -axis lattice parameters for bulk LSCO and LPE films with different Sr contents, respectively, is also shown in Fig. 2(c). We observe that the films suffer an increasingly higher compressive strain along the c axis from $\sim 0.5\%$ in $x=0.081$ to $\sim 0.085\%$ in $x=0.149$, as shown in the secondary y axis. The reason we believe is the increase in lattice mismatch in the films due to anisotropic change in lattice parameters with Sr content in bulk. The films grown by liquid-phase epitaxy are in sharp contrast to films grown by other vapor-phase growth methods, which show strong thickness dependence of strain. From the c -axis compression we could estimate the in-plane lattice strain [Poisson ratio $\nu=0.288$ (Ref. 12)]. The estimated planar constant ($a \times b$) in comparison to that of the bulk LSCOs are shown in Fig. 2(b). We observe excellent lattice planar matching between the LCO substrate and all the films independent of film thicknesses and compositions. From this we can assume that the in-plane lattice expansion of each LSCO film coincides with the relative mismatch between the LCO and that LSCO in bulk. We believe that growth of films at much higher temperatures (above melting points of the flux) and growth near thermoequilibrium conditions are responsible for such strain effects in the films.

Temperature dependence of magnetization (M) for both zero-field-cooled and field-cooled conditions are shown in Fig. 3. A magnetic field of 0.5 mT was applied perpendicular to the film surface (ab plane) for all measurements. We observed that only the LSCO $x=0.081$ sample shows strong diamagnetic signals. However no bulk superconductivity is observed in any other sample. The films of each composition were then cut into strips of different thicknesses. The temperature (T) dependence of the in-plane resistivities (ρ_{ab}) for the LPE films of different compositions and thicknesses are shown in Fig. 4. The measurements were done on the film strips by the conventional four-probe method using a physical property measurement system (PPMS). We observe that only the LSCO films with $x=0.08$ show superconductivity. All other films with higher Sr contents show no superconducting transition down to 2K. In addition to complete destruction of superconductivity in the films with higher Sr contents, the $\rho(T)$ measurements show semiconductorlike be-

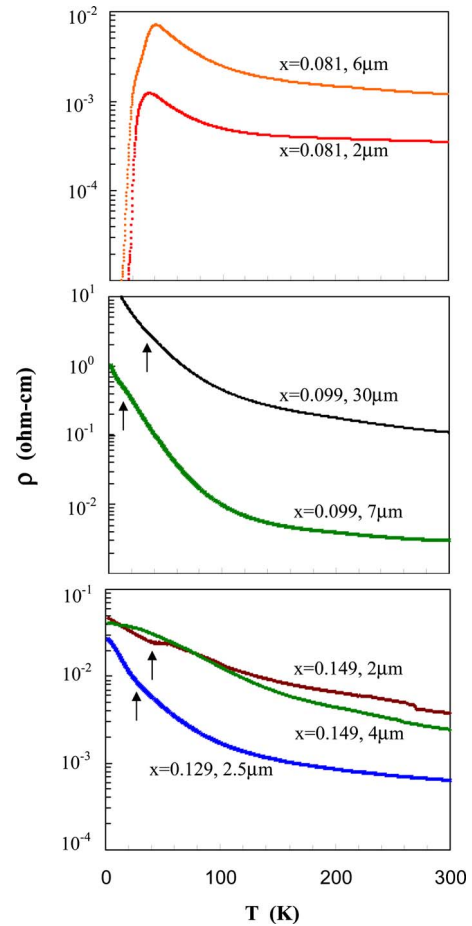


FIG. 4. (Color online) Temperature dependence of resistivities of LSCO films of different thicknesses and Sr content. Filled arrows indicate kink structures in the data.

haviors. We note that the LSCO, $x=0.081$ films suffer smallest strain due to least lattice mismatch [Fig. 2(c)] and the superconductivity although suppressed was not destroyed. Whereas, the disappearance of superconductivity for higher Sr content is correlated with the stronger compressive strain of the c axis due to the tensile strain of the ab plane. We also observe that even the $\rho(T)$ characteristics above 100 K of films are different from typical linear characteristics of in-plane resistivities as observed in bulk. In addition, the change is normal-state resistivity with Sr contents are non-monotonic. We believe that this is due to rather primitive nature of the LPE growth technique. Our method lacks precise control on the parameters that may influence the strained state in the films such as temperature of the substrate at seeding time, temperature gradient near the substrate, temperature of the melt flux, growth speed of film, cooling rate of film after growth, etc. These parameters may vary from one growth to the next, as the human factor is not insignificant. Despite these, we found that, there is excellent reproducibility of ground state whether the film is superconducting or nonsuperconducting for a particular doping, although it can be tricky to grow two films of same composition having exactly identical characteristics in the normal-state resistivity. Structural changes in LSCO systems and their effects on superconductivity are relatively well understood based on

TABLE I. Estimated T_c in LSCO films and LSNCO bulk by uniaxial pressure using strain derivatives from Refs. 1 and 2. (NS: No superconductivity.)

		Estimated T_c compared to experimental values (K)		
La _{2-x} Sr _x CuO ₄ films	$x=0.081$, 2 μm	11.7 (9.5 ^a)		
	6 μm	8.3 (8.5 ^a)		
	$x=0.098$, 7 μm	5.8 (NS)		
	30 μm	6.8 (NS)		
	$x=0.129$, 1 μm	7.3 (NS)		
	2 μm	6.3 (NS)		
	$x=0.149$, 2 μm	13.6 (NS)		
	4 μm	13.6 (NS)		
		$y=0.2$	$y=0.3$	$y=0.6$
LSNCO bulk	$x=0.08$	12.5 (11 ^b)	10.1 (9 ^b)	6.1 (NS)
	$x=0.10$	17.1 (14 ^b)	10.1 (13 ^b)	-3.4 (NS)
	$x=0.15$	29.5 (NS)	24.1 (NS)	13.7 (NS)

^aThis work.

^bReference 9.

several recent studies. Here we have calculated the expected change in T_c in the LPE films using the strain derivatives obtained from study of uniaxial pressure effect on bulk LSCO. Expected T_c of the films are tabulated in Table I. We observe that the estimated T_c of the superconducting samples ($x=0.081$) show reasonable close agreements with the experimental values of T_c . Whereas the uniaxial pressure effect failed to predict the complete destruction of superconductivity in films with $x \geq 0.099$.

It is instructive to compare between anisotropic strains induced by lattice mismatch and that induced by suitable doping of elements. The structural phase transition from the low-temperature orthorhombic (LTO) to the low-temperature tetragonal phase (LTT), as observed in La_{2-x}Ba_xCuO₄ at $x=0.125$, as well as in some rare-earth-doped LSCO is the reason for suppression of T_c and in some cases complete destruction of superconductivity in these materials. It has been found that the LTO to LTT phase transition is actually associated with the rotation ϕ of the tilt axis of the CuO₆ octahedra and the related change in the staggered buckling pattern of the CuO₂ plane.⁸⁻¹⁰ In La_{2-x-y}Sr_xNd_yCuO₄ when ϕ is above a critical angle ϕ_c in the LTT phase, the material goes through a transition from superconducting to a magnetically ordered insulating state. Here we have calculated the expected change in T_c in La_{2-x-y}Sr_xNd_yCuO₄ (LSNCO) due to the anisotropic strain induced by Nd doping in the corresponding LSCO (Table I). We find that, whereas T_c s of superconducting LSNCOs are in reasonable agreements (with in 3 K) with experimental values, as in films the uniaxial pressure effect failed completely to account for $S-I$ transition in LSNCO. This led us to check if the destruction of superconductivity in both materials might have the same origin. In LSNCO the magnitude of ϕ is not only related to the strain along the c axis but also strongly related to the orthorhombic strain in the ab plane. Büchner *et al.*⁹ showed that a critical angle $\phi_c \cong 3.6^\circ$ corresponds to an orthorhombic splitting $\Delta[a-b] \cong 0.035$ Å and a larger orthorhombic splitting leads

to a higher ϕ angle, which is associated with the phase transition to the insulating state. We note that the substrate LCO (001) used for this study in fact has a large orthorhombicity ($\Delta[a-b] \cong 0.048$ Å). Based on our observation in Fig. 2(b) we can assume that the ab planes of the films are strained in a way that the large orthorhombicity in the ab plane of the substrate is mostly translated to that in the films. In order to verify our assumption, we did a detailed x-ray analysis on our thickest sample LSCO, $x=0.01$ (30 μm) which showed no superconductivity despite smallest strain from bulk crystal. Data were taken from the thickest and thinnest part of the film. Measurements were done in the HMI-MAGS synchrotron x-ray beam line in Berlin. With energy 6.2 keV (2 Å wavelength), very close to the La $L1$ edge, we would expect to see no signal from the substrate since transmission through film would be less than 1%. So the exact position of the peaks from substrate and film could be identified at this energy. Measurements were done with photon energies 12.4 keV (1 Å wavelength), where the transmission through 20 μm film is about 30% so that one would expect to see both the film and some part of the substrate. Figure 5 shows typical mesh scans around the (0 2 4) and (2 0 4) reflections. From these we have found that both the a - and b -axis lattice parameter of the film expanded by about 0.5% and c axis contracted by 0.25%. This confirmed that the large orthorhombicity in the film is same as in the substrate.

Now, using the correlation of the suppression of superconductivity with the orthorhombic splitting as given in Ref. 9, we find that the $x=0.081$ film falls in the superconducting $Pccn$ phase. Whereas other films fall in a region in the LTT phase where $\phi_{LTT} > \phi_c$, with no superconductivity. So the predicted superconducting state of all samples is consistent with our results, which also validates the assumption.

It should be added that an SrTiO₃ (001) substrate with a tetragonal structure would act against an orthorhombicity in the ab plane of a film on top.³ This we think is the main reason, apart from strain relaxation, why complete suppres-

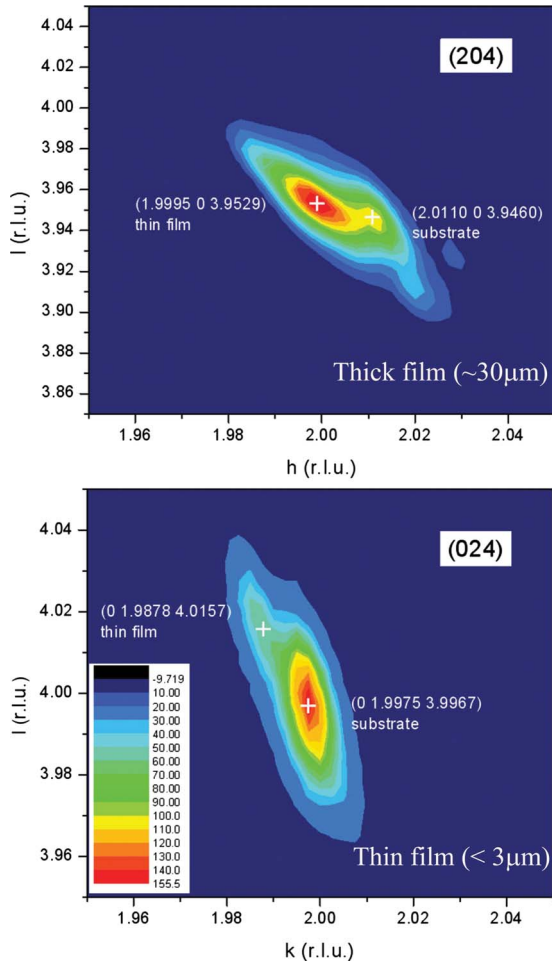


FIG. 5. (Color online) Mesh scans of thickest and thinnest part of LPE films with synchrotron x-ray radiation (HMI-MAGS) around the (2 0 4) and (0 2 4) reflections using photon energy of 12.4 keV.

sion of superconductivity was not observed in previous studies, even though the $(a \times b)$ of STO (30.5 \AA^2) is larger than that of LCO (28.935 \AA^2).

To get a qualitative idea about the change in the CuO_6 octahedra we made comparison of the c -axis strain in the films with that in bulk LSNCO (Ref. 13) and calculated a corresponding effective Nd content for each film for specific Sr contents. In doing so we have assumed that it is possible to describe accurately the nonlinear behavior of the microparameters, such as the buckling of the CuO_6 octahedra, as a function of macro strain, i.e., strain of lattice constants or planes (as concluded in Ref. 14). The effective Nd contents as a function of Sr content of the LPE film are plotted in the phase diagram as given in Ref. 9 (Fig. 6). We observe that this representation could correctly predict the S - I transition, i.e., destruction of bulk superconductivity for films with x

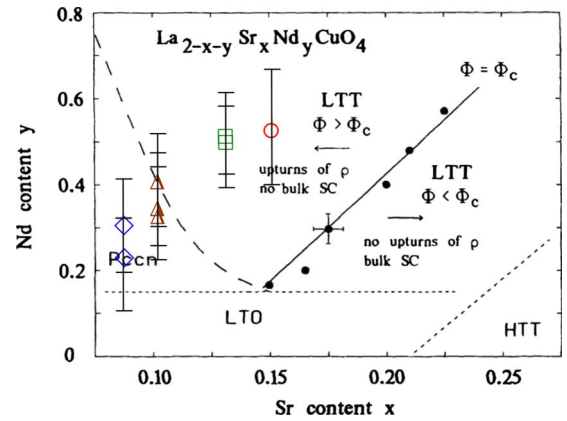


FIG. 6. (Color online) Phase diagram (from Ref. 9) showing correlation between structure and superconductivity in $\text{La}_{2-x-y}\text{Sr}_x\text{Nd}_y\text{CuO}_4$. A scaling of structural change in LPE films with LSNCO can correctly predict the superconducting state in the film.

> 0.08 . The upturn in the $\rho(T)$ measurements as observed in LSNCO samples and predicted by this phase diagram can also be observed in our measurement (Fig. 4). In addition to that, the kink structures in the $\rho(T)$ for $x \geq 0.10$ below 50 K are manifestations of the structural phase transition.¹⁰ Based on these results we believe that the mechanism of S - I transition in LPE films has an identical origin as in LSNCO. Large c -axis compressive strain coupled with an increase in orthorhombic splitting in the ab plane is responsible for a tilting of the CuO_6 octahedra greater than a critical angle ϕ_c in the LTT phase. Now if we consider a $d_{x^2-y^2}$ pairing-state symmetry, large octahedral tilt can act as an effective pair-breaking mechanism. This might be the possible reason for S - I crossover in the LSCO films.

IV. CONCLUSION

In summary, we have grown LSCO single-crystal films in the composition range $0.08 \leq x \leq 0.15$ on La_2CuO_4 (001) substrates by liquid-phase epitaxy method and shown that epitaxial strain is persistent in such films up to several micrometers thicknesses. As effects of such strain we have observed transition from a superconducting state to an insulating state in LSCO, $0.01 \leq x \leq 0.15$ films. We believe that strong orthorhombic strain in the ab plane of the films was crucial for the critical buckling of the CuO_6 octahedra and the superconductor-insulator phase transition.

ACKNOWLEDGMENTS

The authors thank Bella Lake for critical reading of the manuscript. This work had been carried out under the JSPS-UGC (Bangladesh) joint Research Project No. FY2005.

*Corresponding author. nazmul.islam@helmholtz-berlin.de

- ¹F. Gugenberger, C. Meingast, G. Roth, K. Grube, V. Breit, T. Weber, H. Wühl, S. Uchida, and Y. Nakamura, *Phys. Rev. B* **49**, 13137 (1994).
- ²M. Nohara, T. Suzuki, Y. Maeno, T. Fujita, I. Tanaka, and H. Kojima, *Phys. Rev. B* **52**, 570 (1995).
- ³J.-P. Locquet, J. Perret, J. Fompeyrine, E. Machler, J. W. Seo, and G. Van Tendeloo, *Nature (London)* **394**, 453 (1998).
- ⁴H. Sato, M. Naito, and H. Yamamoto, *Physica C* **280**, 178 (1997).
- ⁵I. Bozovic, G. Logvenov, I. Belca, B. Narimbetov, and I. Sveklo, *Phys. Rev. Lett.* **89**, 107001 (2002).
- ⁶H. Sato, A. Tsukada, M. Naito, and A. Matsuda, *Phys. Rev. B* **62**, R799 (2000).
- ⁷I. E. Trofimov, L. A. Johnson, K. V. Ramanujachary, S. Guha, M. G. Harrison, M. Greenblatt, M. Z. Cieplak, and P. Lindenfeld, *Appl. Phys. Lett.* **65**, 2481 (1994).
- ⁸S. Arumugam, N. Mori, N. Takeshita, H. Takashima, T. Noda, H. Eisaki, and S. Uchida, *Phys. Rev. Lett.* **88**, 247001 (2002).
- ⁹B. Büchner, M. Breuer, A. Freimuth, and A. P. Kampf, *Phys. Rev. Lett.* **73**, 1841 (1994).
- ¹⁰T. Noda, H. Eisaki, and S. Uchida, *Science* **286**, 265 (1999).
- ¹¹D. Lampakis, D. Palles, E. Liarokapis, C. Panagopoulos, J. R. Cooper, H. Ehrenberg, and T. Hartmann, *Phys. Rev. B* **62**, 8811 (2000).
- ¹²H. Ledbetter, S. A. Kim, C. E. Violet, and J. D. Thompson, *Physica C* **162-164**, 460 (1989).
- ¹³M. Breuer, B. Büchner, R. Müller, M. Cramm, O. Maldonado, A. Freimuth, B. Roden, R. Borowski, B. Heymer, and D. Wohlleben, *Physica C* **208**, 217 (1993).
- ¹⁴P. Cermelli and P. P.-Guingli, *Physica C* **371**, 117 (2002).